COLLIDING PULSE INJECTION CONTROL IN A LASER-PLASMA ACCELERATOR *

C.G.R. Geddes [†], G.R. Plateau, M. Chen, E. Esarey, N.H. Matlis, D.E. Mittelberger,
K. Nakamura, C.B. Schroeder, Cs. Toth, and W.P. Leemans,
LBNL, Berkeley CA, 94720, USA
E. Cormier-Michel, D.L. Bruhwiler, B. Cowan, and J.R. Cary,
Tech-X, Boulder CO, 80303, USA

Abstract

Control of injection into a high gradient laser-plasma accelerator is presented using the beat between two 'colliding' laser pulses to kick electrons into the plasma wake accelerating phase. Stable intersection and performance over hours of operation were obtained using active pointing control. Dependence of injector performance on laser and plasma parameters were characterized in coordination with simulations. By scanning the intersection point of the lasers, the injection position was controlled, mapping the acceleration length. Laser modifications to extend acceleration length are discussed towards production of tunable stable electron bunches as needed for applications including Thomson gamma sources and high energy colliders.

INTRODUCTION

Laser-plasma accelerators (LPAs) [1] achieve accelerating electric fields thousands of times those of conventional accelerators by using the radiation pressure of an intense laser to drive a plasma wave (review: [2]), or wakefield, whose electric field accelerates particles. Bunches with percent energy spread have been demonstrated at 0.1-1 GeV energies [3, 4] by driving the wake to large amplitude where it traps electrons from the background plasma. In this regime the guiding, wake excitation, and particle trapping are interdependent.

While the energies obtained in LPAs are sufficient for many applications including Thomson gamma sources [5], and staging may be used to address high energy physics applications, tuning of bunch energy and further improvement of momentum spread are needed. To achieve this, several techniques are being used to control injection into the structure, whose wavelength is typically 10's of micron. These include control of the wake phase velocity [6, 7], ionization near the peak laser intensity [8, 9, 10, 11], and colliding laser pulses [12, 13, 14, 15].

In the colliding pulse technique, the ponderomotive force of the beat between two nearly counter-propagating laser pulses is used to capture and inject particles into the accelerating phase of a wake which is operated below the trapping threshold. The strength of the beat is proportional to $a_0 \times a_1$ where $a_{0,1} \propto \sqrt{(I_{0,1})}$ are the normalized vector potentials of the two pulses. The simplest configuration [14] uses a high intensity pulse to drive the wake, and a weaker colliding pulse to inject particles. Because the beat wave should capture particles in a region where there is accelerating field and where plasma density is nonzero, this motivates operation of the wake in a mildly nonlinear to linear regime where the plasma density is not fully blown out by the laser, and with plasma density such that the pulse length is in the range of one plasma period. Three pulse schemes with a separate driver and two injector pulses offer added control [12].

Here we demonstrate stable performance of a two-pulse colliding pulse injector over hours of operation [16], using active laser pointing stabilization to maintain the intersection of the pulses. The plasma density and laser intensity dependence of the injector were characterized, showing that best injection is obtained for parameters consistent with simulated and theoretical expectations. Bunches produced have energies of a few MeV, indicating a short acceleration length. Scanning the location of intersection with respect to the laser axis maps out the acceleration length, which is shown to be of order the laser diffraction range. To provide high energy bunches, laser guiding and a deformable mirror have been implemented to improve laser propagation and mode quality, and to allow scanning of the laser focus.

EXPERIMENTS

Two 45 fs FWHM pulses from the LOASIS Ti:Sapphire laser provided the drive and collider pulses, and were focused to intersect at a 19 degree angle in a 2.2 mm supersonic He or H gas jet target which provided a plasma density adjustable from 0.1 - 30 $\times 10^{18}$/cc density (Figure 1). The pulses collided near the upstream edge of the density plateau, providing maximum acceleration length. The drive pulse was 0.4 J and was focused to $a_0 \sim 3$ in a 5 μm FWHM spot with a Strehl ratio of 0.93. The collider pulse was adjusted from a_1 of 0.1 to 2 in a 6 μm spot. Intersection of the foci of the pulses in the propagation and transverse directions was achieved by overlapping the waists of the ionization contours produced by the two pulses propagating in backfill gas (driver [red] and collider [magenta]

Advanced Concepts and Future Directions
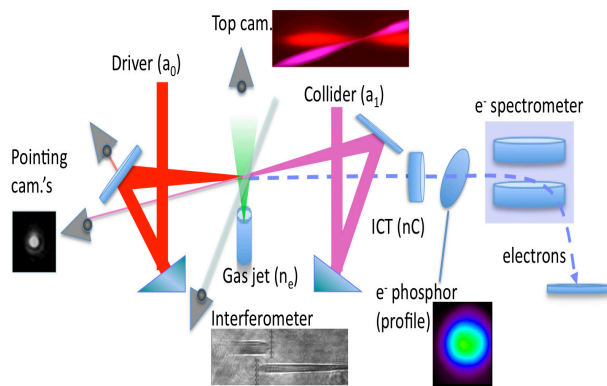
Accel/Storage Rings 14: Advanced Concepts

Figure 1: Setup for colliding pulse controlled injection, showing the drive and collider laser pulses focused on the gas jet, and diagnostics with representative images illustrating alignment and the electron bunch.

shown in Figure 1 top) using a top view camera. Intersection in timing and in the vertical axis was then obtained using a side view interferometer/shadowgram camera and a 50 fs probe pulse (driver [left] and collider [right] in Figure 1 bottom). Electron bunches produced were analyzed using an ICT, phosphor screen, and magnetic spectrometer.

A particular challenge for colliding pulse injection is that overlap of the pulses must be set and maintained within the few μm spotsize and 10's of fs length of the laser pulses. The top and shadow cameras provided initial alignment, and to maintain alignment a camera based active pointing system was implemented. The system incorporates low cost USB and RS170 cameras to correct pointing within the amplifier chain and at the target (target camera locations shown in Figure 1, left). A set of metrics is applied to ensure that the laser spot is of the expected size and shape (this avoids stray light and ensures the system turns off in case of severe misalignment). If these metrics are
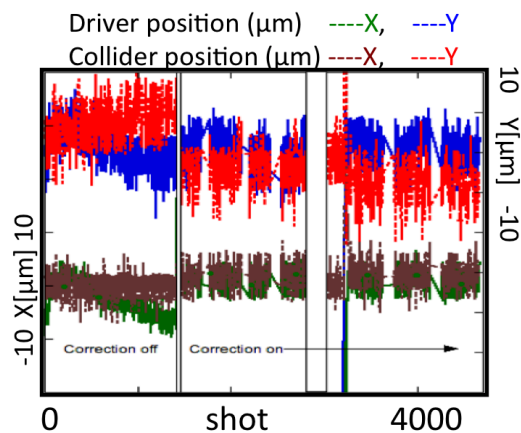

Figure 2: The positions of the drive and collider pulses as monitored on the pointing cameras, without (left) and with (right) active pointing control.
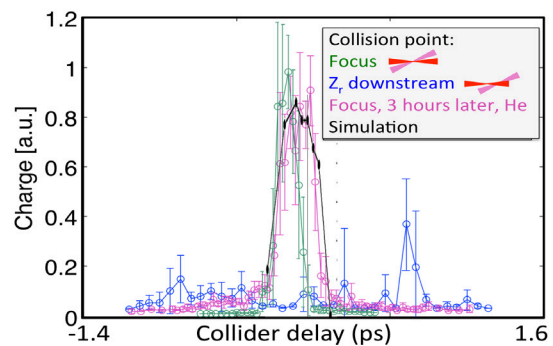

Figure 3: Scan of the collider timing with respect to the driver shows a 200 fs window of overlap region where injection is optimized. Charge stability is $\sim 20\%$. The experimental result agrees well with simulations (which were conducted with $a_1 = 0.5$). Charge versus timing for two different intersection points between driver and collider shows that charge falls off rapidly for intersection $\sim Z_R$ after focus. Performance is repeatable hours later and similar in He and H gas jets.

passed, the centroid location is compared to a target, and commands are sent to the appropriate motors. The system uses TCP communications to serve motor and pointing commands and information across the lab. Figure 2 shows that without active stabilization, pointing drifts by 10 μm over a thousand shots ~ 15 minutes, which resulted in drift of injector performance. With active stabilization pointing is maintained for as long as observed (hour) within a few μm, allowing reliable colliding pulse injector operation as described below. The timing bars in the shadowgram (Figure 1 bottom) are at 50 fs intervals and show that the timing is also maintained within 50 fs over the same period since the pulses originate from the same oscillator and their paths are controlled.

The collider amplitude and plasma density were varied to characterize the parameter dependence of colliding pulse injection. Colliding pulse injection was found to occur above approximately $a_1 = 0.2$, and to plateau near $a_1 = 1$. Injection turned on near $n_e \sim 2 \times 10^{18}$/cc and best operation was obtained for $n_e \sim 4 \times 10^{18}$/cc at which density no self injection was observed. These values are consistent with simulations [17] and with theoretical expectations for the required pulse length relative to the plasma period and for the injection threshold.

The collision timing indicates that the beating of the colliding pulses, and not wake-wake interactions, are responsible for injection. The timing window (Figure 3) of 200 fs matches simulations and is understandable as the time over which the pulses, propagating at 19 degrees to one another, no longer overlap. Successive scans over three hours of operation show repeatable injection, with charge repeated to the few percent level, indicating a reliable injector and effectiveness of the active laser pointing control. The electron bunches produced (Figure 4) are near 3 MeV, indicat-
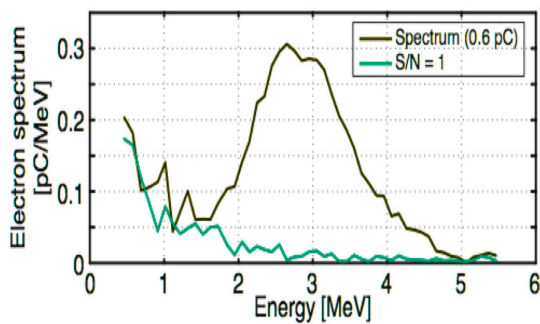
Advanced Concepts and Future Directions

Accel/Storage Rings 14: Advanced Concepts

Figure 4: Energy spectrum of the colliding pulse injector, showing a bunch at 3 MeV with chage of 0.6 pC.

ing a short acceleration length.

Pulse collision position in the plasma regulates the location at which electrons are injected into the wake, and was used to map the length of the accelerator structure. Figure 3 shows that moving the collision point by about a diffraction range Z_R leads to a sharp falloff in charge, indicating that the wake is not excited over a long distance. This was confirmed by Thomson side scatter and interferometry measurements, which indicated that the pulse remained focused over $\sim Z_R$, and hence that self focusing was not effective in maintaining the laser focus. Simulations indicate that a Gaussian laser can self focus for these conditions [17], motivating improvement of the laser mode.

To extend interaction length for higher electron bunch energies, a deformable mirror and laser guiding have been implemented. The deformable mirror, together with laser chain optimization, has resulted in a near diffraction limited spot with Strehl ratio ~ 0.97 (Figure 5), reducing optical aberrations which can disrupt propagation. In addition, via control of wavefront curvature, the focal position can be scanned axially, facilitating alignment and mapping of the accelerator as shown in Figure 3. Laser preformed channels have also been implemented to extend propagation. Similarly to those reported in [3], use of these channels have produced 90 MeV bunches in self trapped experiments. In
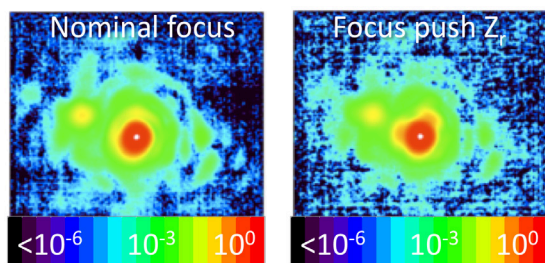

Figure 5: Drive laser focal spot (log scale) shows nearly Gaussian performance with Strehl ratio near 0.97. Implementation of a deformable mirror allows the axial position of the focus to be adjusted (right) while maintaining spot quality, facilitating scans such as those in Figure 3.

the present implementation no long pulse heater laser was used, which is anticipated to allow formation of channels at low plasma densities as required for colliding pulse injection.

CONCLUSION

Experiments demonstrated repeatable operation of a colliding pulse optical injector for an LPA by using active pointing control of the laser to maintain pulse intersection. Reliable operation over hours was obtained, with $\sim 20\%$ charge stability. Timing, density and collider amplitude scans are consistent with simulations and with the expected scalings for colliding pulse. It was shown that the low energy of the resulting bunches was due to limited acceleration length. Laser modifications have increased mode quality, and provided the capability to scan intersection, and plasma guiding has been implemented to increase focused propagation length. Future experiments will apply these techniques towards high energy bunches from colliding pulse injection. Simulations indicate that combining guiding with colliding pulse, 200 - 400 MeV bunches of 10's of pico-coulombs of charge and narrow energy spread relevant to Thomson gamma sources may be produced from a compact 10 TW laser.

REFERENCES

[1] T. Tajima and J. M. Dawson, Phys. Rev. Lett. **43**, 267 (1979).

[2] E. Esarey, C. B. Schroeder, and W. P. Leemans, Rev. Mod. Phys. **81**, 1229 (2009).

[3] C. G. R. Geddes et al., Nature **431**, 538 (2004).

[4] W. P. Leemans et al., Nature Physics **2**, 696 (2006).

[5] C. Geddes et al., Proc. CAARI, AIP Conf. Proc **1099**, 666 (2008).

[6] S. Bulanov et al., Phys. Rev. E **58**, R5257 (1998).

[7] C. G. R. Geddes et al., Phys. Rev. Lett. **100**, 215004 (2008).

[8] M. Chen et al., Journal of Applied Physics **99**, 056109 (2006).

[9] T. P. Rowlands-Rees et al., Phys. Rev. Lett. **100**, 105005 (2008).

[10] C. McGuffey et al., Phys. Rev. Lett. **104**, 025004 (2010).

[11] A. Pak et al., Phys. Rev. Lett. **104**, 025003 (2010).

[12] E. Esarey et al., Phys. Rev. Lett. **79**, 2682 (1997).

[13] H. Kotaki et al., Phys. Plasmas **11**, 3296 (2004).

[14] G. Fubiani et al., Phys. Rev. E **70**, 016402 (2004).

[15] J. Faure et al., Nature **444**, 737 (2006).

[16] G. R. Plateau et al., AIP Conference Proceedings **1299**, 180 (2010).

[17] E. Cormier-Michel et al., These Proceedings .